Rhodium(II) Dimers Without Metal-Metal Bonds

Di Zhu,*[a] Arzoo Z. Sharma,[c] Christopher R. Wiebe[b] and Peter H.M. Budzelaar[c]

a) State Key Laboratory of Heavy Oil Processing, College of Science, China University of Petroleum, Beijing 102249, P.R. China. email: dizhu@cup.edu.cn.
b) Department of Chemistry, University of Winnipeg, 515 Portage Ave, Winnipeg, MB R3B 2E9, Canada.
c) Department of Chemistry, University of Manitoba, Winnipeg, MB R3T 2N2, Canada.

Experimental details

General:

All experiments were carried out in a nitrogen-filled dry-box or under an argon atmosphere using standard Schlenk techniques. Hexane, pentane, toluene, toluene-d_8, tetrahydrofuran, THF-d_8, and cyclohexane were distilled from sodium/benzophenone.

^{1}H NMR spectra were recorded on Bruker Avance 300 MHz and Bruker Avance 500 MHz spectrometers. All ^{1}H NMR shifts (δ, ppm) were referenced to the solvent (toluene-d_8: $C_6D_5CD_2H$ δ 2.08; $CDCl_3$,: $CHCl_3$ δ 7.26; THF-d_8: OC*H*D δ 3.58). COSY spectra were also acquired to assist ^{1}H assignments. Elemental analysis was done at Guelph Chemical Laboratories Ltd, Canada. Lithium salt (^{Me}BDI)Li(THF) was prepared according to literature procedures.[1] Iodine, bromine and other reagents were purchased from Aldrich or Acros. $[Rh(COE)_2Cl]_2$ was purchased from Strem Chemicals and used as received.

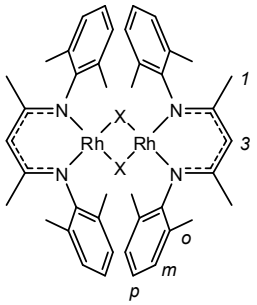

[(^{Me}BDI)Rh]$_2$(μ-I)$_2$·toluene (1a·toluene)

In a N_2-filled dry box, $[(COE)_2RhCl]_2$ (0.0718g, 0.100 mmol) and (^{Me}BDI)Li(THF) (0.0768g, 0.200 mmol) were weighed into a small vial, and 5 mL dry THF was added. After vigorous shaking for 5 minutes, the color of the mixture turned clear brown. This solution was transferred to a 25 mL Schlenk tube. After being kept at room temperature for 1h, this brown solution was evaporated to dryness *in vacuo* and the resulting residue was extracted with dry cyclohexane (3 mL). After centrifugation, the cyclohexane solution was evaporated to dryness *in vacuo* to furnish a solid. This solid was dissolved in 10 mL dry THF and cooled to -78 °C. At this temperature, a solution of I_2 in THF (0.90 mL, 0.1 mol/L, 0.090 mmol) was added dropwise. The resulting mixture was allowed to warm to -8 °C over 30 minutes (the color turned green at around -56 °C), and kept at -8 °C for 1hr. The green solution was evaporated to dryness *in vacuo* and the resulting green residue was extracted with dry toluene (3 mL) in the dry-box. After centrifugation, this green toluene solution was layered with hexane and cooled to -35 °C overnight, and a dark crystalline solid was deposited. The mother liquor was pipetted off, leaving 0.0275 g of a

crystalline solid (yield 24%). One crystal of this batch was used for single-crystal X-ray diffraction. The X-ray structure showed one disordered molecule of toluene per dimer, but NMR spectra taken of vacuum-dried samples indicated the presence of only about 0.8 toluene per dimer. Presumably, the toluene of crystallization is only loosely bound and easily lost on drying.

^{1}H NMR (THF-d_8, 300 MHz): δ 23.67 (8H, br, $\Delta\nu_{1/2}$ 20 Hz, NAr *m*), 14.43 (4H, br, $\Delta\nu_{1/2}$ 18 Hz, NAr *p*), 7.06-7.18 (~4H, m, toluene C*H*), 2.30 (~2.4 H, s, toluene CH_3), 2.42 (24H, br, $\Delta\nu_{1/2}$ 31 Hz, NAr CH_3), -36.87 (12 H, br, $\Delta\nu_{1/2}$ 32 Hz, *1*), -153 (br, 390 Hz, *3*).

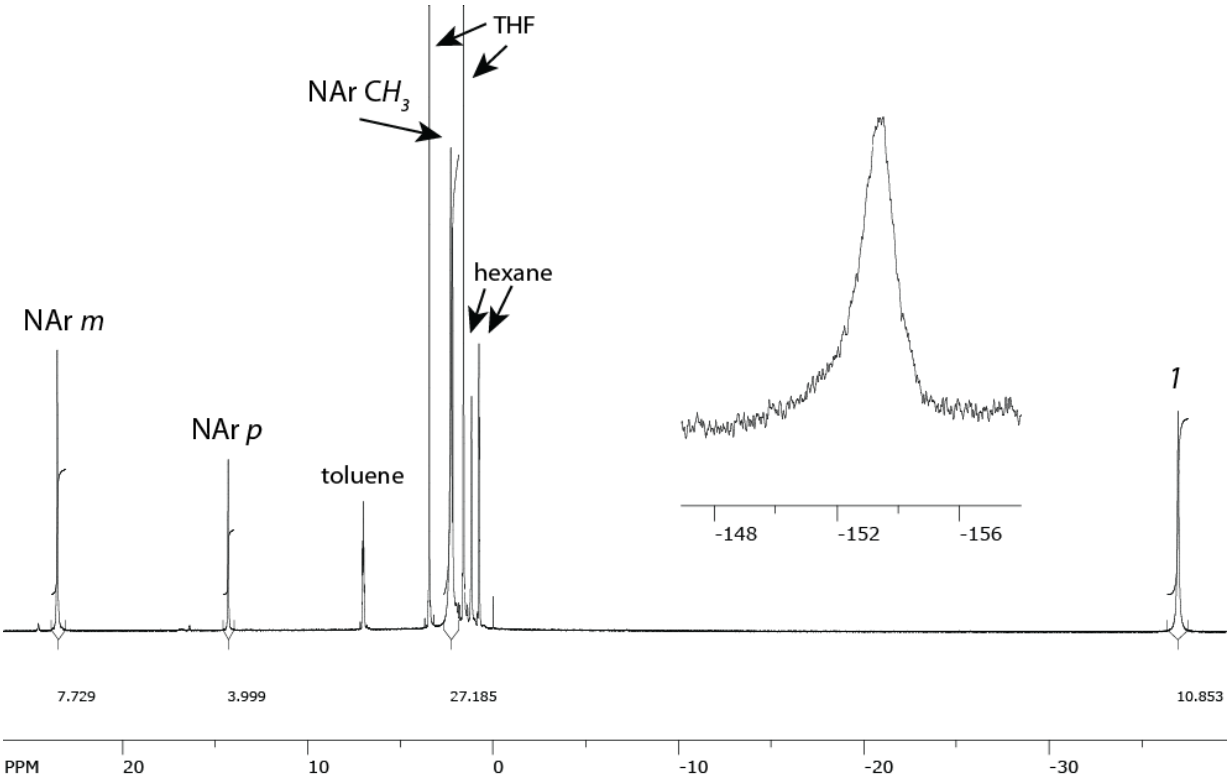

Figure S1. ^{1}H NMR spectrum of 1a.

Anal. Calcd for $C_{49}H_{58}I_2N_4Rh_2$ (1162.63): C, 50.62; H, 5.03; N, 4.82. Found: C, 50.66; H, 5.22; N, 4.76.

Magnetic moment

Evans method:[2-4] In a dry box, **1a**·toluene (0.0120 g, 0.01mmol) was dissolved in a mixture of 0.2 mL dry THF-d_8 and 0.1 mL dry THF. A small part of this dark green solution was added into the inner tube of a concentric NMR tube and one drop of toluene, 0.1 mL THF (reagent grade) and 0.3 mL dry THF-d_8 were added into the outer tube. This NMR sample was measured on a 500 MHz NMR machine at T = 300.1 K. Δδ of the THF peaks was determined as 1.31 ppm (655Hz), yielding a μ_{eff} of 4.5(3) μ_B.

Direct measurement: The DC magnetic susceptibility was measured using a Quantum Design Physical Property Measurement System (PPMS) with an applied field of 0.1 T in the temperature range 1.8 K - 300 K. Hysteresis scans were also completed up to applied fields of 9 T. Magnetometry was done under vacuum, with a trace of helium gas.

[(^{Me}BDI)Rh]$_2$(μ-Br)$_2$·toluene (1b·toluene)

In a nitrogen-filled dry box, [(COE)$_2$RhCl]$_2$ (0.0348g, 0.0485 mmol) and (^{Me}BDI)Li(THF) (0.0373g, 0.0970 mmol) were weighed into a small vial, and 5 mL dry THF was added. After vigorous shaking for 5 minutes, the color of the mixture turned clear brown. This brown solution was evaporated to dryness *in vacuo* and extracted with dry hexane (3 mL). After centrifugation, the hexane solution was evaporated to dryness *in vacuo* to generate a solid. This solid was further dissolved in 10 mL dry THF and cooled to -78 °C. At this temperature, a freshly prepared Br_2 solution in THF (0.14 mL, 0.3 mol/L, 0.0448 mmol) was added dropwise. The resulting mixture was allowed to warm to -10 °C over 30 minutes, and the solution color turned bright green. At this temperature, this green solution was evaporated to dryness *in vacuo*. The resulting green residue was extracted with dry toluene (3 mL). After centrifugation, this green toluene solution was layered with hexane and cooled to -34 °C overnight. Dark green crystalline solids precipitated. The green mother liquor was pipetted off, leaving (0.010g) of a dark green crystalline solid. One crystal of this was used for single-crystal X-ray diffraction measurement. The mother liquid was further concentrated and layered with hexane at -34 °C overnight. More solid (0.022 g) was isolated by pipetting off the mother liquor. Combined yield: 64% (relative to starting material [(COE)$_2$RhCl]$_2$).

^{1}H NMR (THF-d_8, 300 MHz): δ 31.13 (8H, br, $\Delta\nu_{1/2}$ 25 Hz, NAr *m*), 18.54 (4H, br, $\Delta\nu_{1/2}$ 19 Hz, NAr *p*), 7.08-7.19 (~6H, m, toluene C*H*), 2.30 (~3.6 H, s, toluene CH_3), 1.98 (24H, br , $\Delta\nu_{1/2}$ 121 Hz, NAr CH_3), -55.40 (12 H, br, $\Delta\nu_{1/2}$ 46.2 Hz, *1*), *3* not observed.

Anal. Calcd for $C_{49}H_{58}Br_2N_4Rh_2$ (1068.63): C, 55.07; H, 5.47; N, 5.24. Found: C, 54.79; H, 5.21; N, 4.91.

X-ray structure Determinations

General

Crystal fragments were broken from large pieces of crystalline aggregates and sealed in a thin glass capillary. The crystal fragment in its capillary was mounted on a Bruker D8 three-circle diffractometer equipped with a rotating anode generator (Mo *K*α X-radiation), multi-layer optics incident beam path and an APEX-II CCD detector. Data were collected at a crystal-to-detector distance of 5 cm and processed using the Bruker SMART suite.[5] Semi-empirical absorption corrections (SADABS[6]) were applied and identical data merged. The unit-cell parameters were obtained by least-squares refinement on observed reflections with $I > 4\,\sigma(I)$. Structures were solved using SHELXS and refined using SHELXL.[7] Hydrogens were put at calculated positions and refined in riding mode. Details of the individual determinations are given in Table S1.

1a·toluene

A dark green crystal fragment (0.20×0.20×0.30 mm) was used. The crystal contained a second component, but this did not appear to overlap badly and did not affect the measurement significantly. In excess of a sphere of X-ray diffraction data (44029 reflections) was collected to 2θ = 60° using 6 s per 0.3° frame. Data merging produced 14227 reflections covering the Ewald hemisphere. The unit-cell parameters were obtained by least-squares refinement on 9848 reflections. The toluene molecule is disordered and is located over a centre of inversion. It was refined using constrained bond lengths, with a fixed total occupation factor of 1.0.

1b·toluene

A dark green crystal fragment (0.30×0.30×0.40 mm) broken from the large aggregate was used. In excess of a sphere of X-ray diffraction data (45034 reflections) was collected to 2θ = 60° using 4 s per 0.3° frame. Data merging produced 13867 reflections covering the Ewald hemisphere. The unit-cell

parameters were obtained by least-squares refinement on 9474 reflections. The toluene molecule is disordered and is located over a centre of inversion. It was refined using constrained bond lengths, with a fixed total occupation factor of 1.0. This compound is virtually isostructural with **1a**·toluene.

Table S1. Details of crystal structure determinations.

Complex	**1a·toluene**	**1b·toluene**
Formula	$C_{49}H_{62}I_2N_4Rh_2$	$C_{49}H_{62}I_2N_4Rh_2$
Mol wt	1166.65	1072.67
T (K)	293(2)	293(2)
Crystal system	Monoclinic	Monoclinic
Space group	C2/m	C2/m
a / Å	19.268(7)	18.862(7)
b / Å	11.773(4)	11.848(5)
c / Å	14.410(4)	14.220(5)
α/ deg	90	90
β/ deg	131.886(6)	131.564(13)
γ/ deg	90	90
V / Å^3	2433.4(14)	2377.7(16)
Z	2	2
D_c / g cm^{-3}	1.592	1.498
abs coef / mm^{-1}	1.982	2.411
F_{000}	1160.0	1088.0
index ranges	$-23 < h < 23$ $-14 < k < 14$ $-17 < l < 17$	$-22 < h < 22$ $-14 < k < 14$ $-17 < l < 17$
$2\theta_{max}$ / deg	51	51
# rflctns	9067	8868
# unique	2396	2336
# > 2σ	2256	2251
GOF	1.082	1.050
# parameters	150	151
R ($Fo > 4\ \sigma(F)$)	0.0279	0.0347
R (all data)	0.0294	0.0358
$wR2$ (all data)	0.0897	0.1042
largest peak, hole / e Å^{-3}	0.768, -0.645	1.031, -0.689

Table S2. Selected bond distances (Å) and angles (°) in the solid state structures of 1a, 1b and $[(Ph)(^{Me}BDI)Rh]_2(\mu\text{-}Br)_2$.[8]

	1a·toluene	**1b·toluene**	$[(Ph)(^{Me}BDI)Rh]_2(\mu\text{-}Br)_2$
Rh(1)-N(1)	2.003(4)	1.993(4)	2.013(6)
Rh(1)-N(2)	2.008(4)	1.996(4)	2.026(6)
Rh(1)-X(1)	2.6420(11)	2.4921(9)	2.5211(8)
Rh(1)-X(1')	2.6449(9)	2.4939(11)	2.5255(9)
N(1)-C(12)	1.328(6)	1.321(7)	1.278
N(2)-C(14)	1.332(6)	1.322(7)	1.311
Rh(1)-Rh(1)	4.057(1)	3.819(2)	3.827
X(1)-X(1')	3.390(1)	3.205(2)	3.290
N(1)-Rh(1)-N(2)	89.85(15)	90.07(17)	90.3(3)
N(1)-Rh(1)-X(1)	174.83(10)	174.88(11)	172.23(17)
N(2)-Rh(1)-X(1)	95.33(11)	95.05(12)	93.65(18)
X(1)-Rh(1)-X(1')	79.756(19)	80.02(4)	81.38(3)
Rh(1)-X(1)-Rh(1')	100.24(2)	99.98(4)	98.62(3)
N(2)-N(1)-X(1')-X(1)	(0)	(0)	3.20

Table S3. Structurally characterized transition metal $[(BDI)M]_2(\mu\text{-}X)_2$ complexes.

Core	Ligand[a]	Description[c]	Ref
Cr_2Cl_2	^{iPr}BDI	square planar, slightly stepped	9
Cr_2Cl_2	^{iPr}BDI-tBu	square planar, twisted	10
Mn_2Cl_2	^{iPr}BDI	tetrahedral, stepped	11
Mn_2Br_2	^{Et}BDI	tetrahedral, slightly twisted	12
Mn_2I_2	^{iPr}BDI	tetrahedral, stepped	13
Fe_2F_2	^{iPr}BDI	intermediate, perfectly twisted, a bit stepped	14
Fe_2Cl_2	^{iPr}BDI	tetrahedral, stepped	15
Fe_2Br_2	(2,4,6-$Ph_3C_6H_2$)-BDI	tetrahedral, twisted	16
Co_2Cl_2	^{iPr}BDI	tetrahedral, stepped	17
Ni_2Cl_2	^{Me}BDI	tetrahedral, stepped	18
Ni_2Cl_2	^{iPr}BDI	tetrahedral, stepped	19
Ni_2Br_2	^{Me}BDI-CF_3	tetrahedral, twisted	20
Cu_2Cl_2	^{Me}BDI - β-Cl[b]	intermediate, perfectly twisted	21
Cu_2Cl_2	^{Cl}BDI	intermediate, perfectly twisted, a bit stepped	22
Cu_2I_2	^{Me}BDI	intermediate, stepped	23
Zn_2F_2	^{Me}BDI	tetrahedral, stepped	24
Pd_2Cl_2	^{H}BDI	square planar, stepped	25
Pd_2Cl_2	(3,5-$(CF_3)_2C_6H_3$)-BDI	square planar, stepped	26
Pd_2Cl_2	^{iPr}BDI	square planar, slightly stepped	26

[a] Abbreviations used: ^{R}**BDI**: 2,6-$R_2C_6H_3$ groups at N; **X-BDI**: X groups at N; **BDI-Z**: Z groups instead of CH_3 groups at imine carbons. [b] Cl instead of H at central carbon of BDI. [c] For deformations see below.

Schematic representations of deviations from perfect D_{2h} symmetry:

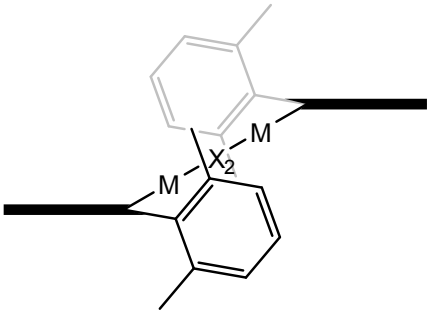

Stepped

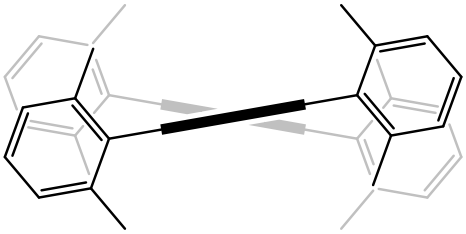

Twisted

Computational details

All transition state structures were fully optimized at the (restricted or unrestricted) b3-lyp[27-29]/TZVP[30, 31] level using Turbomole[32] coupled to an external optimizer (PQS OPTIMIZE[33, 34]). Some calculations were also done with the b-p functional[35, 36] (the Turbomole "b3-lyp" and "b-p" functionals are similar, but not identical, to the "B3LYP" and "BP86" functionals commonly used with versions of Gaussian). The nature of each stationary point was checked with an analytical second-derivative calculation (no imaginary frequency for local minima; exactly one imaginary for each transition state). The vibrational analysis data were also used to calculate thermal corrections (enthalpy and entropy, 298 K, 1 bar) for all species considered using the standard formulae of statistical thermodynamics. Calculations were performed for a simplified β-diiminate model (Me groups at N) as well as the real ^{Me}BDI ligand (2,6-$Me_2C_6H_3$ groups at N). The spin density plot was prepared using Molden.[37]

Table S4. Comparison of X-ray structures and unrestricted DFT optimized geometries for 1a.

	1a·toluene	**1a, S = 1 b3-lyp/TZVP**	**1a, S = 0 b3-lyp/TZVP**	**1a, S = 1 b-p/TZVP**	**1a, S = 0 b-p/SV(P)**	**1a, S = 0 b-p/TZVP**
$\langle S^2 \rangle$		**2.0155**	**0.9955**	**2.0109**	**0.8209**	**0**
Rh1-N1	2.003(4)	2.043	2.043	2.018	2.026	2.018
Rh1-N2	2.008(4)	2.043	2.043	2.018	2.025	2.018
Rh1-X1	2.6420(11)	2.762	2.758	2.735	2.725	2.704
Rh1-X1’	2.6449(9)	2.762	2.757	2.737	2.724	2.703
N1-C12	1.328(6)	1.333	1.333	1.345	1.351	1.345
N2-C14	1.332(6)	1.334	1.334	1.345	1.351	1.345
Rh1-Rh1	4.057(1)	4.232	4.232	4.208	4.223	4.190
X1-X1’	3.390(1)	3.548	3.535	3.498	3.444	3.416
N1-Rh1-N2	89.85(15)	90.53	90.55	90.93	91.06	91.01
N1-Rh1-X1	174.83(10)	165.22	165.51	165.34	173.17	166.80
N2-Rh1-X1	95.33(11)	96.45	96.39	96.39	95.33	96.50
X1-Rh1-X1’	79.756(19)	79.94	79.73	79.46	78.41	78.37
Rh1-X1-Rh1’	100.24(2)	99.98	100.23	100.51	101.58	101.63
N1-N2-X1-X1’	(0)	20.26	-19.80	20.01	-3.79	-17.34

Brief discussion:

Rh-N bond lengths are best reproduced by with the b-p functional. Calculated Rh-I distances are too large with both functionals, but the b-p values are closer to the X-ray structure. Bond lengths within the organic ligands are better reproduced by b3-lyp. This agrees with observations by Minenkov.[38] Angles in the Rh_2I_2 core are very similar for both functionals. Only b-p in combination with the small SV(P) basis produced the pseudo planar structure of the dimer; use of the TZVP basis and/or b3-lyp functional resulted in a 20° twist of the two monomers relative to each other that reduces steric repulsion between the $Me_2C_6H_3$ side arms of the two monomers. However, the potential energy surface for this twist is extremely flat; the planarity of the X-ray structure might even be caused by packing forces rather than intrinsic preference. Most other $[(^{R}BDI)M]_2(\mu\text{-}X)_2$ complexes show some form of distortion from planarity, see Table S3.

Model diiminate: energies and Rh-Rh distances

DFT calculation on the model system (Table S5) indicate that the triplet state (**A**) is a lower in energy (4.83kal/mol) than the open-shell (broken-symmetry) singlet or (4.41 kcal/mol) the close-shell singlet. The predicted Rh-Rh distance of complex in triplet state is much closer to the X-ray structure. Structure **B** is a triplet with a Rh-Rh bond (this structure does not exist for the full system).

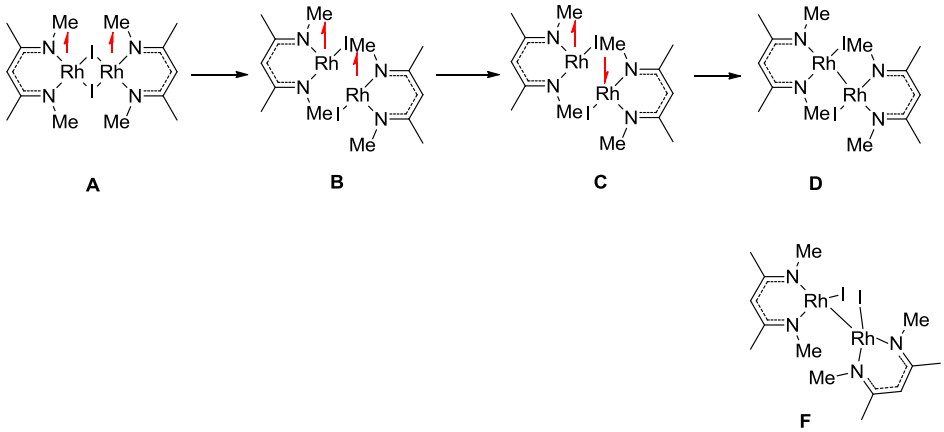

Figure S2. Alternative arrangements for model BDI complexes.

Table S5. Rh-Rh distances (Å) and relative energies (kcal/mol) for complexes of model diiminates.

Arrangement:	**A**	**B**	**C**	**D**	**F**
Rh-Rh distance	4.206	2.623	2.548	2.547	2.727
E_{rel} (b3-lyp/TZVP)	(0)	9.34	4.81	8.92	2.44
G_{rel} (b3-lyp/TZVP)	(0)	7.03	4.83	8.28	4.41
$<S^2>$	2.01	2.02	0.45	(0)	(0)

Full ^{Me}BDI system: energies and Rh-Rh distances

The energies of triplet **A'** and open-shell (broken-symmetry) singlet **C'** are predicted to be almost same (Table S6). *Both* feature a large Rh-Rh distance, which indeed indicates that repulsion of the β-diiminate ligands plays a significant role in determining the Rh-Rh bond length. A closed-shell optimized structure (**D'**) is much higher in energy and still doesn't have the Rh atoms within bonding distance.

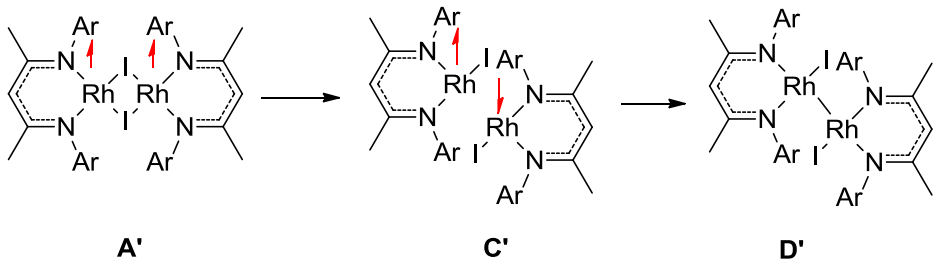

Figure S3. Alternative arrangements for ^{Me}BDI complexes.

Table S6. Rh-Rh distances (Å) and relative energies (kcal/mol) for ^{Me}BDI complexes.

Arrangement:	A'	C'	D'
Rh-Rh distance	4.232	4.232	4.196
E_{rel} (b3-lyp/TZVP)	(0)	-0.50	18.13
G_{rel} (b3-lyp/TZVP)	(0)	-0.10	19.10
$<S^2>$	2.02	0.99	(0)

Comparison: energies and Rh-Rh distances for $[Cp^*Rh]_2(\mu\text{-}Cl)_2$

In contrast to **1a**/**1b**, $[Cp^*Rh]_2(\mu\text{-}Cl)_2$ has a direct bond between two rhodium centers. For comparison we studied the energies and geometries for this system with and without Rh-Rh bond. The results (Table S7) indicate that geometries with and without metal-metal bond are very close in energy.

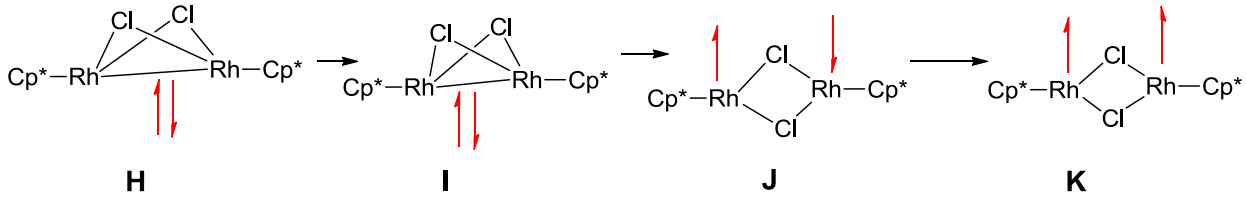

Figure S4. Alternative arrangements for Cp* complexes.

Table S7. Rh-Rh distances (Å) and relative energies (kcal/mol) for Cp* complexes.

Arrangement:	H	I	J	K
Rh-Rh distance	2.649	2.675	3.531	3.455
E_{rel} (b3-lyp/TZVP)	(0)	-0.04	1.86	1.79
G_{rel} (b3-lyp/TZVP)	(0)	-0.88	-1.67	-0.24
$<S^2>$	(0)	0.12	1.01	2.01

Formation of complex 1a (Scheme 2)

Table S8. Total energies and thermal corrections (b3-lyp; a.u.) and <S^2> values for species in Scheme 2 in the main text.

Species	<S^2>	E(TZVP)	Therm[a]	G(TZVP)
(^{Me}BDI)Rh(COE) (**A**)	(0)	-1348.20431	0.54654	-1347.65777
I_2	(0)	-22.80725	-0.02530	-22.83255
Intermediate **B**	0.00	-1371.01842	0.53757	-1370.48086
COE	(0)	-313.14506	0.17227	-312.97280
Intermediate **E**	0.00	-1371.02653	0.54202	-1370.48452
Intermediate **C**	0.60	-1057.87641	0.34051	-1057.53590
Intermediate **D**	0.00	-1057.90665	0.34451	-1057.56215
[(^{Me}BDI)Rh]$_2$(μ-I)$_2$ (**F**)	2.02	-2092.98924	0.72078	-2092.26846

[a] gas phase, 1 bar, 298 K.

Table S9. Calculated relative free energies (kcal/mol) for species in Scheme 2 in the main text.

Species	ΔG_{rel}[a]
(^{Me}BDI)Rh(COE) (**A**)	(0)
Intermediate **B**	5.94
Intermediate **E**	3.64
Intermediate **C**	-11.53
Intermediate **D**	-28.01
[(^{Me}BDI)Rh]$_2$(μ-I)$_2$ (**F**)	-41.39

[a] gas phase, 1 bar, 298 K.

References

1. P. H. M. Budzelaar, N. N. P. Moonen, R. de Gelder, J. M. M. Smits and A. W. Gal, *Eur. J. Inorg. Chem.*, 2000, 753-769.
2. D. F. Evans, *Journal of the Chemical Society*, 1959, 2003-2005.
3. E. M. Schubert, *J. Chem. Educ.*, 1992, **69**, 62-62.
4. S. K. Sur, *J. Magn. Reson.*, 1989, **82**, 169-173.
5. *Smart program suite 6*: Bruker, Bruker AXS Inc, Madison, Wisconsin
6. *SADABS*G. M. Sheldrick, University of Göttingen, Germany, 1996
7. G. M. Sheldrick, *Acta Crystallogr., Sect. A: Found. Crystallogr.*, 2008, **64**, 112-122.
8. S. T. H. Willems, P. H. M. Budzelaar, N. N. P. Moonen, R. de Gelder, J. M. M. Smits and A. W. Gal, *Chem. Eur. J.*, 2002, **8**, 1310-1320.
9. V. C. Gibson, C. Newton, C. Redshaw, G. A. Solan, A. J. P. White and D. J. Williams, *Eur. J. Inorg. Chem.*, 2001, 1895-1903.
10. H. Fan, D. Adhikari, A. A. Saleh, R. L. Clark, F. J. Zuno-Cruz, G. Sanchez Cabrera, J. C. Huffman, M. Pink, D. J. Mindiola and M.-H. Baik, *J. Am. Chem. Soc.*, 2008, **130**, 17351-17361.
11. J. F. Chai, H. P. Zhu, H. W. Roesky, C. He, H. G. Schmidt and M. Noltemeyer, *Organometallics*, 2004, **23**, 3284-3289.
12. S. Yao, Y. Xiong and M. Driess, *Chem. Eur. J.*, 2012, **18**, 11356-11361.
13. J. F. Chai, H. P. Zhu, K. Most, H. W. Roesky, D. Vidovic, H. G. Schmidt and M. Noltemeyer, *Eur. J. Inorg. Chem.*, 2003, 4332-4337.
14. J. Vela, J. M. Smith, Y. Yu, N. A. Ketterer, C. J. Flaschenriem, R. J. Lachicotte and P. L. Holland, *J. Am. Chem. Soc.*, 2005, **127**, 7857-7870.
15. N. A. Eckert, J. M. Smith, R. J. Lachicotte and P. L. Holland, *Inorg. Chem.*, 2004, **43**, 3306-3321.
16. R. E. Cowley and P. L. Holland, *Inorg. Chem.*, 2012, **51**, 8352-8361.
17. W. Gao, Y. Mu, G. H. Li, X. M. Liu, Q. Su and W. Yao, *Chem. Res. Chin. Univ.*, 2005, **21**, 240-242.
18. H. L. Wiencko, E. Kogut and T. H. Warren, *Inorg. Chim. Acta*, 2003, **345**, 199-208.
19. N. A. Eckert, E. M. Bones, R. J. Lachicotte and P. L. Holland, *Inorg. Chem.*, 2003, **42**, 1720-1725.
20. Y. Li, L. Wang, H. Gao, F. Zhu and Q. Wu, *Appl. Organomet. Chem.*, 2006, **20**, 436-442.
21. D. J. E. Spencer, A. M. Reynolds, P. L. Holland, B. A. Jazdzewski, C. Duboc-Toia, L. Le Pape, S. Yokota, Y. Tachi, S. Itoh and W. B. Tolman, *Inorg. Chem.*, 2002, **41**, 6307-6321.
22. S. Wiese, Y. M. Badiei, R. T. Gephart, S. Mossin, M. S. Varonka, M. M. Melzer, K. Meyer, T. R. Cundari and T. H. Warren, *Angew. Chem., Int. Ed.*, 2010, **49**, 8850-8855.
23. M. M. Melzer, S. Mossin, X. Dai, A. M. Bartell, P. Kapoor, K. Meyer and T. H. Warren, *Angew. Chem., Int. Ed.*, 2010, **49**, 904-907.
24. H. J. Hao, C. M. Cui, H. W. Roesky, G. C. Bai, H. G. Schmidt and M. Noltemeyer, *Chem. Commun.*, 2001, 1118-1119.
25. A. Hadzovic and D. Song, *Organometallics*, 2008, **27**, 1290-1298.
26. V. T. Annibale, R. Tan, J. Janetzko, L. M. Lund and D. Song, *Inorg. Chim. Acta*, 2012, **380**, 308-321.
27. A. D. Becke, *J. Chem. Phys.*, 1993, **98**, 5648-5652.
28. A. D. Becke, *J. Chem. Phys.*, 1993, **98**, 1372-1377.
29. C. T. Lee, W. T. Yang and R. G. Parr, *Phys. Rev. B*, 1988, **37**, 785-789.
30. F. Weigend, F. Furche and R. Ahlrichs, *J. Chem. Phys.*, 2003, **119**, 12753-12762.
31. A. Schäfer, C. Huber and R. Ahlrichs, *J. Chem. Phys.*, 1994, **100**, 5829-5835.
32. *TURBOMOLE V6.3*: TURBOMOLE GmbH, since 2007, Karlsruhe, 2011
33. *PQS 2.4*: J. Baker, Parallel Quantum Solutions, Fayetteville, AR, 2001
34. J. Baker, *J. Comput. Chem.*, 1986, **7**, 385-395.
35. A. D. Becke, *Phys. Rev. A*, 1988, **38**, 3098-3100.
36. J. P. Perdew, *Phys. Rev. B*, 1986, **33**, 8822-8824.

37. G. Schaftenaar and J. H. Noordik, *J. Comput.-Aided Mol. Des.*, 2000, **14**, 123-134.
38. Y. Minenkov, A. Singstad, G. Occhipinti and V. R. Jensen, *Dalton Trans.*, 2012, **41**, 5526-5541.